16th International Conference on Space Operations, Cape Town, South Africa - 03 - 05 May 2021.

SpaceOps-2021,12,x1548

Layout and Design of a pressurised Structure for gelled Propellants for a Thrust controllable Sounding Rocket Upper Stage

Maximilian Zurkaulen [a]*

[a] *Mobile Rocket Base of the German Aerospace Center, Münchener Str. 20, 82234 Weßling, Germany, maximilian.zurkaulen@dlr.de*
* Corresponding Author

Abstract

In-situ measurements in middle and higher atmosphere regions are often only possible by means of sounding rockets. The typical trajectory of a sounding rocket is a suborbital, elliptic flight path which practically leads to only several seconds during ascent as well as descent to perform the desired measurements. To improve scientific gain and provide longer measurement times in the relevant altitude regions, the Mobile Rocket Base (MORABA) and partners of the German Aerospace Center as well as industrial partners are working on a thrust controllable upper stage for sounding rocket applications. The upper stage will be powered by a gelled propellant engine and enable the payload to hover on a certain altitude level or perform different, non-ballistic flight paths. To achieve this, it will be equipped with an attitude control system consisting of a thrust vector control unit for the engine and additional cold gas thrusters. In this way, it would be possible to precisely target atmospheric phenomena and perform local measurements with an essentially extended local operating time in comparison to current sounding rocket concepts. The rocket engine will be pressure fed by the propellant tank system which is a key element of the upper stage, providing a sufficient fuel flow and pressure needed for the optimal combustion and different thrust levels.
This paper concentrates on the development of a fuel tank for gelled propellants for the supply of the upper stage engine. The development process is described from defining the task over the concept development to a detailed CAD model concept. The peculiarities of this tank are the light and economical design as well as the integrated, pressure driven piston to feed the propellant. The focus of this work is the definition of the concept and the subsequent structural FEM analysis of the tank system.
Keywords: concept development, FEM, high pressure structure, propellant tank design, sounding rocket

1. Introduction

Although there are several rocket motors developed for sounding rocket applications, typically sounding rockets have been and still are based on a military standard that are equipped with scientific equipment [1,2]. Whereas in the beginning of sounding rocketry also a couple of liquid propellant rockets have been used, nowadays mostly solid propellant motors are in service [2]. This is mainly due to the fact that most military rockets and missiles that could be converted into sounding rockets use solid fuels as well [3]. Solid propellant motors have the great advantage of a long storage time and easy handling. Despite these very useful features, they hardly be throttled during flight. The main way to tailor the performance of a solid rocket motor is to change the propellant mixture or geometry to direct the burn rate [3]. For some experiments which require a specific operation altitude, like some atmospheric measurements, this means that there is a window of a couple seconds on the ascent of the vehicle as well as on the descent to perform the measurements. To be able to provide longer operating times in certain altitudes regions a thrust controllable engine is necessary. To meet this demand the Mobile Rocket Base of the German Aerospace Center and industrial partners set the goal to develop a thrust controllable upper stage for sounding rockets. The Mobile Rocket Base (MORABA), based in Oberpfaffenhofen is a department of the Space Operations and Astronaut Training of the German Aerospace Center. The name tag "mobile" is derived from the ability to theoretically launch sounding rockets anywhere on the earth. Therefore, the first mobile campaign was launched in Greece in May 1966. Since then almost 500 campaigns have been launched all around the world. Besides NASA, MORABA is the only institution in the western hemisphere that is capable of launching high altitude research mission anywhere in the world [4].

There are several types of thrust controllable engines using different propellants. Due to the demand for simple handling, any cryogenic propellant constellation is considered unattractive. Because of the size and mass of a hybrid, a single propellant system is favoured and due to their toxic properties monergolic catalytic propellants are not pursued any further. In this project it finally leads to a gelled propellant which is decomposed thermically in the burning chamber. The gelled propellant has the advantage to be easy in handling, no toxicity and it is a single propellant/oxidiser material combination [5]. The gel is to be stored in a tank and fed into the burning chamber. Due

to their complexity and the properties of the gel, turbopumps are not considered. Therefore the tank needs to offer the function to feed the propellant out of the tank and into the engine for example through pressure feeding. There are several technical solutions to do so which will be discussed further on. The aim of this paper is to define a concept and design for the mentioned propellant tank system. The tank will have the function to store the propellant, to feed it into the piping system leading to the engine and it has to withstand structural loads of the rocket since it will be an integral part of the primary vehicle structure. The use of gelled propellants is comparably new in rocketry and therefore little other applications are known. Besides some demonstrators for missile applications, gelled propellants have not been used in sounding rockets yet. Therefore no existing optimised tanks for flight hardware are available.

2. Concept of the Gelled Propellant Tank Structure

2.1 General Vehicle Design

The current vehicle concept consists of a booster stage and the new gel engine upper stage. With an acceleration of approximately 20 g, the booster will burn for a few seconds and accelerate the upper stage to the desired altitude level of around 80 km. During the ascent the vehicle will spin up in order to reduce dispersion. After the booster burn phase and the following coast phase without propulsion, the yo-yo de-spin is performed to remove the vehicle's spin. Stage separation will follow afterwards and prepare the upper stage flight. Figure 1 shows the current design of the upper stage propulsion system including the gel tank and the already implemented pressure feed gas system.

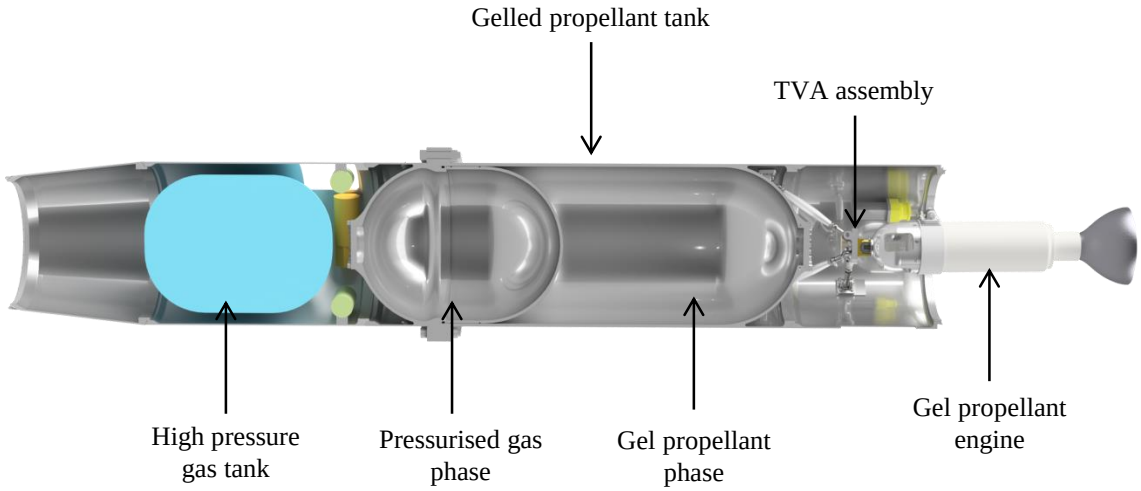

Figure 1: Upper stage propulsion system

2.2 Expected loads and load cases on the structure

There are many different loads and a few relevant load cases the structure will have to withstand during its service time. However, in this paper only loads of operation are discussed since they are the driving loads on the structure. Fatigue cases are not examined since the service life of this tank is considered short without the requirement of reusability. In the following, Table 1 shows the different loads on the tank with the corresponding operational cases.

	Transverse force	Axial force	Bending moment	Torsional moment	Pressure	Thermal load
Test on ground, filled, with pressure					**Internal pressure** 12 N/mm²	**Outside temperature** neglectable
Test on ground, integrated, filled, with pressure		**Payload weight** 2453 N			**Inernal pressure** 12 N/mm²	**Outside temperature** neglectable
Flight with Booster , integrated, filled, with pressure	**Inertial loads + Aerodynamic loads** 8635 N	**Inertial loads + Aerodynamic loads** 40732 N	**Inertial loads + Aerodynamic loads** 26412 Nm	**Inertial loads** 455 Nm	**Inernal pressure** 12 N/mm²	**Thermal protection** neglectable
Flight upper stage , integrated, filled, with pressure		**Inertial loads** 4286 N			**Inernal pressure** 12 N/mm²	
Re-entry , integrated, empty, no pressure	**Inertial loads** neglectable	**Inertial loads** neglectable	**Inertial loads** neglectable			**Thermal protection** neglectable
Recovery , integrated, empty, no pressure			**Inertial loads** neglectable			

Table 1: Loads on the tank

Although the ascent during booster burn might seem like the worst case condition, single loads can act compensating to each other. This means that the internal pressure will create some tensile stresses in the structure whereas the thrust and the inertial forces of the upper part will induce some compressive stresses. This combination is relieving. Therefore, the single not-relieving loads are put together for a worst case consideration and design of the structure.

Three load cases are created. The first load case showing tensile stresses is represented by the internal pressure of the tank on the ground with a load factor of 1.5. During booster flight, for maximum tensile stresses the pressurised tank under bending loads is considered as load case two and for maximum compressive stresses the depressurised tank with aerodynamic and inertial forces is considered as load case three. In order to also validate any twisting, shear stresses are added to load case two for maximum tensile stress since this will be the more critical case. Table 2 shows the mentioned load cases.

Load case	Load type	Value	Unit	Load factor
1 (on ground)	Internal pressure	18	N/mm²	1.5
2 (flight – mainly tensile stresses)	Internal pressure	15	N/mm²	1.25
	Bending moment	26.4	kNm	1.33
	Transverse force	8635	N	1.33
	Torsional moment	605	Nm	1.33
	Inertia of the gel	24.5	kN	1.25
3 (flight – mainly compressive stresses)	Axial load	40732	N	1.33
	Bending moment	26.4	kNm	1.33

Table 2: Load cases

The internal pressure with a maximum expected operating pressure of 12 N/mm² and the load factor of 1.5 results in the dominating load for this application. The load factors are described in detail in section 2.4.

2.3 Key Design Requirements

The most important design requirements are the fixed outside diameter of 438 mm and the fixed propellant volume. The constraint on the external diameter refers to the re-use of existing subsystems and modules for this vehicle. Also since the tank will be a part of the primary structure of the vehicle, the interface to other modules is of importance. Therefore it has to be designed with so called Radax connections on the top and bottom. Further on it is necessary to differentiate between a prototype model and a small series version. Since this is the first design of the tank structure and it has not been built before, some extra features are to be implemented to provide for minor adaptations once it has already been built. These features are mainly flanges and adapter plates. To provide options for different connections and interfaces for gas and gel, adapter plates have to be included in the top and in the bottom.

2.4 Relevant Technical Standards for Aerospace Engineering

In engineering the use of standards gives safety to the designer, providing a guideline on how to layout and on where safety margins are needed for an adequate level of reliability. Although this gel tank is a prototype and for the moment presents a feasibility study, the relevant standards are outlined. They can be divided into technical standards for specific design and size of mechanical parts and some which present necessary factors of safety. The specific standards for example for the design of cylindrical shaped structures under internal pressure are described in the according sections. In this section, the focus lies on determining the necessary factors of safety for the structure. For aerospace applications the European Cooperation for Space Standardization (ECSS) provides some relevant development guidelines. The structural design and verification of pressurised hardware [6] has to be taken as a guideline for pressurised hardware. This standard presents definitions and necessary factors of safety for pressurised structures. Besides that, another ECSS guideline exists, providing guidelines for factors of safety for general loads for spaceflight hardware [13]. According to the ECSS, the relevant pressure type definition for the tank is a pressurised structure since it will have to carry internal pressure as well as structural loads of the rocket. Page 34 of [6] explains the required factors of safety for internal pressure. The question which factor should be applied is not trivial. Since the sounding rocket is an unmanned vehicle, the factors of safety for unmanned missions should be taken into consideration. Although, when the rocket is getting ready for launch, mounted on the launch rail, it needs to be possible to encounter the potentially pressurised tank. In the moment when somebody approaches the rocket it cannot be considered unmanned any more. To have the flexibility of pressurising the tank before launch and to have a certain factor of safety for ground operations a different factor (FOSU) for internal pressure is chosen. The ECSS suggests a minimum factor of safety ultimate in manned missions of 1.4, however MORABA decided to increase the factor to 1.5. Table 3 shows the applied factors for the corresponding flight phases.

Mission phase	**Load**	**FOSY**	**FOSU**
On ground	MEOP	1.25	1.5
In flight	MEOP	1.1	1.25
	Additional flight loads	1.1	1.33

Table 3: Factors of safety

Here FOSY is the "Factor Of Safety Yield" and FOSU is the "Factor Of Safety Ultimate". Therefore considering the previously mentioned aspects the factor of safety ultimate for ground operations is set to 1.5 and the factor for yield during ground operations is set to 1.25 by definition of MORABA. During the flight when no human is close to the rocket and several other loads apply the necessary factors of safety are lowered. The factor of safety ultimate is set to 1.25 and the factor for yield during flight to 1.1 as they are stated in the ECSS [6].

The other applicable loads during flight are covered in the ECSS of Structural factors of safety for spaceflight hardware [13]. The required minimum factors of safety for metallic parts of launch vehicles are set to 1.1 for FOSY and 1.25 for FOSU according to ECSS. The internal MORABA safety factor on these loads was increased to 1.33. The presented factors of safety are calculated to load factors according to the ECSS [6]. The obtained load factors are applied on the previously shown loads that provoke tensile stresses and the driving load is analysed. The driving load is the internal

pressure of 18 N/mm² in the ground case (load case one). Therefore the design process is oriented on the internal pressure according to load case one. Afterwards all load cases are applied independently on the FEM- model and analysed.

3. Concept design

3.1 Choice of Material and corresponding Wall Thickness

The general concept design of the propellant tank includes the condition of a pressurised tank as an integral structure, a piston to separate the gas and propellant and an option non-destructively open the tank, a flange. Therefore, the choice of material has a significant impact on the design. The material choice is based on strength, density, stiffness, availability, price, complexity of engineering and the complexity of manufacturing. The aim is to find a material with a high material strength and low density resulting in a high specific strength in order to reduce as much mass as possible. Additionally the stiffness, availability and price should be reasonable as well as the engineering and manufacturing for the tank as simple as possible. Between these aspects a trade-off has to be made in order to find the most suited material for this project. On one hand it should be as light as possible but also as strong as possible. This would potentially lead to fibre enforced materials like carbon fibre for example. Although it has a very high specific strength, carbon fibre is more complicated to design, since it needs precise positioning of the fibres, evenly distributed resin in a well-defined fibre/resin ratio. According to MORABA philosophy of simple manufacturing for this prototype, any fibre material is excluded. This leads to metallic materials that can be machined at the commonly collaborating machine shops. Table 4 shows the properties of three chosen representative metallic alloys. A high strength Aluminium alloy, a Steel alloy for highest strength applications and a widely used high strength Titanium alloy have been chosen [7]. These three are chosen because they represent a broad spectrum of different type metallic materials. Aluminium is very commonly used in lightweight applications, Titanium also although it has an even higher specific strength than Aluminium and the Steel as comparison since it has a much higher strength than both of the other alloys. Typical pressure tank steels are not used since the strengths of these steels are below the chosen materials and rather suitable for ground based long-lifetime use cases.

Material	**Strength [N/mm²]**	**Yield strength [N/mm²]**	**Density [g/dm³]**	**spec. strength [kNm/kg]**	**Young's modulus [N/mm²]**
Aluminium	482	413	2,8	172	71000
Steel	1860	1815	8.2	227	210000
Titanium	895	828	4.45	201	114000

Table 4: Material parameters

These values are used for all following calculations. In order to calculate the wall thickness for the cylindrical part of the tank, the technical standard DIN EN 13445-3 is considered [8]. With help of the formula 1 for cylindrical shells the wall thicknesses of the cylindrical part and with the help of equation 2 the corresponding mass for each of the three materials are calculated. The applied pressure is the internal pressure with a value of 18 N/mm² including the mentioned design and safety factors of 1.5 as described before. The outside diameter De is 438 mm and the factor f represents the maximum stress which is set to the ultimate strength of each material since the previously described safety factor is against ultimate stress. Z is the factor for welding which is set to z = 1 since there are no welds. The length for the mass calculation is set to 1 m as it is not known yet how for example the bottom shape will be. The results of this calculation are shown in Table 5.

$$e = \frac{P*De}{2f*z+P} \tag{1}$$

$$m = V\rho = AL\rho = \left[\frac{De^2}{2} - \frac{De-2e^2}{2}\right]\pi * L\rho \tag{2}$$

Obviously, the resulting wall thickness for the Steel alloy is the lowest with 2.11 mm, followed by the thickness for Titanium with 4.36 mm and lastly Aluminium with 8.18 mm. Taking the masses into consideration the specific strength

already predicts the differences. Therefore, the Steel cylinder has the lowest mass, followed by Titan and Aluminium. However the total difference in mass is roughly 7 kg between steel and aluminium which is about 25 %.

Material	**Cyl. wall thickness [mm]**	**Cyl. Mass [kg]**
Aluminium	8.18	30.93
Steel	2.11	23.69
Titanium	4.36	26.43

Table 5: Cylindrical wall thicknesses and corresponding masses

In order to build the tank, different approaches can be pursued. It can be designed as an integral part, resulting in high material costs but with the possibility of manufacturing of complex structures. Requests at manufacturers and forges have also shown that it is possible to die forge a "pot" that could afterwards be milled down. A pot is a cylinder with one bottom where much less material is wasted compared to a massive block. Alternatively, it is possible to use flat sheets, bending and welding them together. Table 6 shows advantages and disadvantages of the three different materials, also in handling and working with the materials in a qualitative manner.

Material	**Advantages**	**Disadvantages**
Aluminium	Cheap Simple manufacturing No need for welding	Lowest specific strength Low Young‘s modulus
Steel	Highest specific strength Highest Young‘s modulus	Highest density Welding is necessary
Titanium	High specific strength	More difficult manufacturing Very expensive

Table 6: Advantages and disadvantages of the materials

The Steel alloy requires a welding process since the high strength is only achievable in thin sheets through heat treatment. Welding is not encouraged due to the thermal distortion and weakening of the material with the thin wall thicknesses. This will add a higher complexity and call for potential upscaling of the wall thickness. Also, the inside of the cylinder contact surface would have to be machined again to ensure a smooth running of the piston. The flat sheets are also disadvantageous considering the sphere-shaped bottom since the sheet will have to be reshaped for which a specialized forming tool would be needed. Hence, any need of welding is considered rather critical and the preferred process is milling the structure out of a "pot" shape. Considering the high price of Titanium for manufacturing and the material itself, the Aluminium alloy is the preferred way to go even though it has the lowest specific strength.

3.2 Bottom Design

This subsection deals with the design of the bottoms on both sides of the tank. Various bottom designs are presented and necessary wall thicknesses calculated. After that, the obtained results are numerically analysed in section 4.2.2. The design of bottoms or also referred to as heads is driven by the internal pressure on one side and the request for low mass and volume on the other side. Four different bottom types are investigated. The list below shows the type of bottom including the connected technical standard:

- flat bottom (iteratively designed by testing in ANSYS)
- half-sphere bottom (DIN EN 13445-3)
- Torispherical heads (DIN EN 13445-3 and DIN 28011)
- Ellipsoidal heads (DIN EN 13445-3 and DIN 28013)

The following Figure 2 shows the shape of these four heads according to the standards.

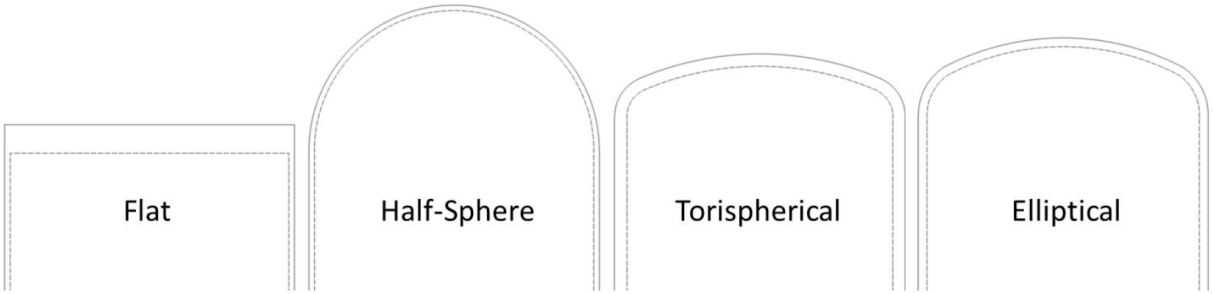

Figure 2: Comparison of bottom types

Each bottom is calculated by applying corresponding technical standards and afterwards analysed in detail. The tank design consists of the cylindrical shape of the tank and two bottoms on the ends. To investigate the influences of the y-joint to the attached structure modules one bottom of the tank is equipped with the specific interface for the FEM analysis. According to the standard, the torispherical and elliptical bottoms have a cylindrical part before the curvature in the same thickness like the curvature itself. This is assumedly to avoid bending moments. Therefore, the whole cylindrical part is designed in the same wall thickness as the bottom to avoid any interferences.

The flat bottom is the most basic form of bottom shapes, it is not adapted for pressurised structures like the other types therefore it is expected to be the most heavy of all options. The technical standard applied for this bottom type is the section VIII of the American Society of Mechanical Engineers (ASME). This technical standard covers fired and unfired pressure vessels [9]. Applying this standard leads to a calculated wall thickness for the flat bottom of 81.48 mm. This leads to a mass of roughly 33.15 kg which is unacceptable concerning the mass budget. Thus, the flat bottom is not considered any further.

In comparison to the flat bottom, the half-sphere bottom induces less bending moments by diverting all loads into tensile stresses. Therefore, the wall thickness can be kept the lowest of all the bottoms as it can be seen in the comparison in Table 7. On the other hand the total volume of this bottom is much higher than the other ones. The half-sphere bottom is designed according to DIN EN 13445-3 [8]. The equation results out of the formula for shell structures under internal pressure also known as Barlow's law. It is extended by the weld factor z and is transformed to be calculated with the external diameter De. The wall thickness is represented by the variable e, the internal pressure by P and the material strength by f. The used values as well as the calculated thickness are shown in Table 7 resulting in a needed wall thickness for the half-sphere bottom of 4.09 mm.

A compromise between the two options can be found in the other adapted bottom types for pressurised structures, the torispherical and elliptical bottoms. The torispherical as well as the elliptical bottom are specially adapted bottom designs to keep the needed build volume lower than the half-sphere bottom and to reduce the bending moment of the flat bottom type significantly. The bottoms are designed according to the technical standards described in the table above. Like the half-sphere bottom, the torispherical bottom is also covered by DIN EN 13445-3 for the calculations and additionally DIN 28011 for the design and construction [10]. The results of the calculations are shown in Table 7. The technical standards used here are all primarily written for unalloyed, low-alloyed or non-corroding steels. However, it is explained, that if the bottoms are of different shapes or materials the standards apply correspondingly with tolerances that have to be defined specially. Therefore, and due to the fact that no specific technical standard was found during the research of this paper which would cover aluminium bottoms directly, these technical standards are used.

Character	Half-sphere Value	Torispherical Value	Elliptical Value	Flat Value	Unit
P	18	18	18	18	N/mm²
De	438	438	438	438	mm
f	482	482	482	482	N/mm²
e	4.09	18.9	7.11	81.48	mm

Table 7: Used factors and results of the bottom calculations

As it can be seen in Table 7, the minimum required wall thickness for the torispherical bottom is 18.9 mm. Since the torispherical bottom requires a cylindrical part with the same thickness as the curvature, the integration on the main cylinder with the much smaller wall thickness proves to be difficult. This would mean material extending on the outside of the tank interfering with the flange or on the inside interfering with the piston. Therefore the torispherical bottom is not considered any further. Only the half-sphere as well as the elliptical bottom are analysed in with FEM in the following chapter. There however it is expected that the elliptical bottom won't show sufficient results with the calculated wall thickness since the standard was not very clear in this point and the structure is very similar to the torispherical bottom.

4. FEM Analysis

This chapter deals with the numerical analysis of the tank concept presented in chapter 3. The analysis will be performed using the program ANSYS R19.2. A static structural analysis is performed.

4.1 General Model Properties

For the materials, the previously described Aluminium alloy is used for the main structure as well as a high strength Steel for the bolts, nuts and washers. The adapted values can be seen in the following Table 8.

	Tensile Yield N/mm²	Tensile Ultimate N/mm²	Compressive Yield N/mm²	Young's modulus N/mm²
Aluminium	413	482	434	71000
Steel	900	1100	1080	210000

Table 8: Engineering data

The geometry of each different model for the analysis is built in Autodesk Inventor 2016 and transferred to the ANSYS Workbench. The mesh is generated in the ANSYS internal auto meshing feature. Whereas solid elements have a volume and can be suited better to analyse big volumetric parts, shell elements can be more useful for thin-walled structures. Although thin-walled structures can also be computed with solid elements, shell elements can be more efficient since the element size can be chosen much higher than for solid elements. Besides the needed surface-model in order to use shell elements, special care has to be taken for "T"-connected shell elements since the information cannot always be transported properly [11]. For the more complicated flange analysis where it is inevitable to use solid elements. Solid elements however are limited to the structure thickness concerning especially the thin cylindrical wall. With elements getting smaller, the total amount of necessary elements can rise very quickly and impact computational performance significantly. In order to determine if the usage of solid elements is justified, a short comparison between shell and solid elements is performed. Therefore, the basic model of the cylindrical centre part and the two half-sphere bottoms with a wall thickness of 8.18 mm each is used. The model is meshed one time with solid tetrahedral elements and another time with triangular shell elements using the same element size. This way the maximum elemental mean equivalent stress, is analysed and compared. The following Table 9 shows the obtained stress according to the element size for each element type. Also the deviation of each is given for comparison.

Element	**100**	**50**	**20**	**10**	**8**	**5**	**4**	**[mm]**
Shell	458,42	435,1	434,05	432,12	431,9	431,83	431,77	[N/mm²]
Solid	433,99	424,4	424,45	423,89	427,34	427,87	429,45	[N/mm²]
Deviation	5,63	2,52	2,26	1,94	1,07	0,93	0,54	%

Table 9: Element comparison

As it can be seen, the difference between shell and solid is marginal and decreasing with a decreasing element size. Also, the result converges within the different element types with reducing size. Therefore, it can be concluded that with 8.18 mm of wall thickness the usage of solid elements with edges up to 10 mm is justified since it shows a deviation of less than 2%. Therefore, the used elements are quadratic tetrahedral elements with a maximum size of 10 mm. Additionally to this, a simple convergence check is performed for each following analysis in order to rule out any other unexpected potential side effects of the mesh. If the result does not vary more than 5 % to the previous, it is considered sufficient.

4.2 Analysis of the Tank Structure

This section presents the analysis of the tank structure using the FEM simulation. The obtained results of section 3.2 are implemented into a CAD model and then analysed. The numerical model is validated on the simple geometries of the cylindrical wall thickness and the bottoms. Subsequently the model is adapted with every step adding the main flange and flanges on the bottoms to analyse the more complex geometries. Therefore, it can be concluded that the models to analyse the more complex structures are sufficient and working correctly with a certain accuracy. In the end the final model is built in CAD and simulated in FEM for the remaining factors of safety. The used forces are according to the critical load cases as described earlier.

4.2.1 Analysis of the cylindrical Part

For analysis of the basic tank geometry, a model without any flanges or connections is built with the wall thickness of 8.18 mm according to section 3.2. The aim is to verify the FEM results for a basic pressure containment with a cylindrical center. The half sphere bottoms are used in this case to avoid bending moments in the structure induced by the applied loads. The internal pressure of 18 N/mm² is used and applied on the complete internal surface of the model. The highest stresses are in the cylindrical part as it is intended. The maximum equivalent Von-Mises stress lies at 432.89 N/mm². The difference to the 482 N/mm² material strength which were used in the analytic design lies in the displayed stress type. Since Von-Mises is an equivalent stress it takes into account the axial and as well the lower circumferential stresses. When the maximum principle stress is considered, the highest value reaches 475,99 N/mm², very close to the 482 N/mm². However, another ten measurement points are taken with an average of 417.14 N/mm² Von-Mises equivalent stress. This shows that the stress is very consistent over the whole cylindrical area. An additional mesh convergence study shows that there is no significant change in stresses. The difference of a mere 1.2 % is achieved by dividing the element size by half to 5 mm. Therefore the wall thickness of 8.18 mm for the cylindrical part is kept for the following analyses.

4.2.2 Analysis of the Bottom Shape

As described previously there are only two different bottom shapes for pressurised structures remaining, the half-sphere and the elliptical bottom. According to the previously made calculations of the existing technical standards for each of the described bottoms a model is built and analysed. In the following, the different bottoms are discussed in further detail.

The half-sphere bottom was calculated analytically to a wall thickness of 4.09 mm before. Therefore a tank with two half-sphere bottoms and the according thickness is built with the cylindrical part as described before. One side of the bottoms is fitted with a skirt, a cylindrical part extending over the bottom, to simulate the further needed Radax joint. The fixed support of the model is connected to the structural adapter on one of the bottoms and the internal pressure of 18 N/mm² is set to all internal surfaces. The results of this analysis are shown in the following Figure 3 on the left side. As it can be seen in the figure, the stresses surpass the strength of the aluminium alloy of 482 N/mm². This is exceeded in multiple areas by far. Mainly the transition area to the cylinder is concerned. There it does not matter if it is the free side or with the cylindrical skirt. The challenge is the jump in material thickness. The stresses can reach up to almost 600 N/mm² on the free side and 522 N/mm² on the skirt side. It could be argued to include a

more suited transition from the extending cylindrical wall to half-sphere bottom in order to avoid these stresses. However the wall thickness is so thin that every additional bending stress surpasses the limit of 482 N/mm². Therefore, as the last iteration, the wall thickness for the half-sphere bottom is kept at the same as the cylindrical wall resulting in a maximum stress of 246.5 N/mm². In comparison to the 10 mm elements, a mesh of 5 mm elements shows a difference of merely 0.89 %.

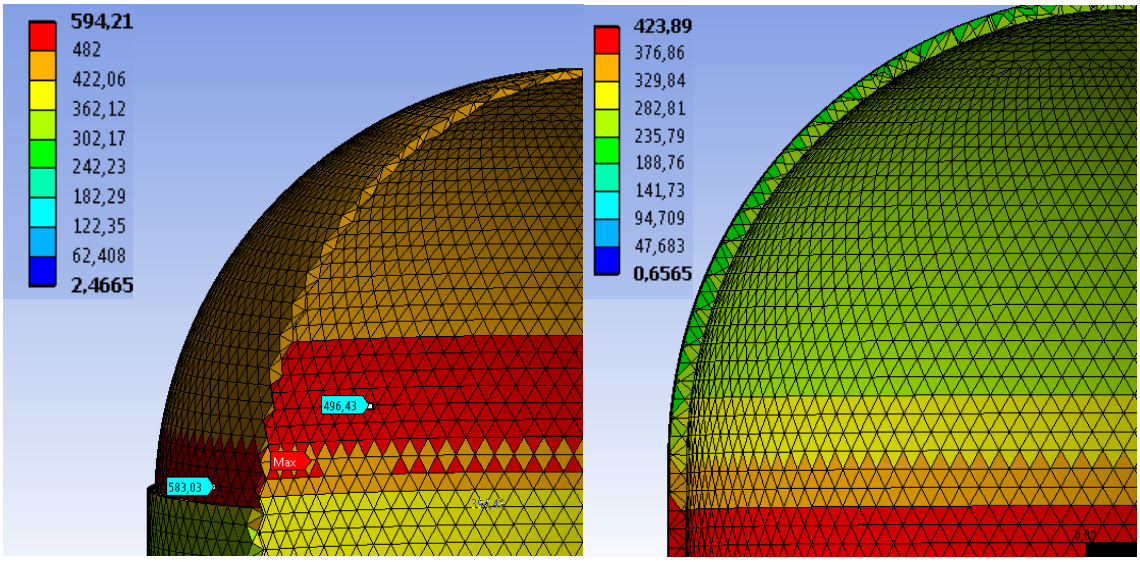

Figure 3: Half-sphere bottom with a wall thickness of 4.09 mm – and with a wall thickness of 8.18 mm

The elliptical bottom is designed with a wall thickness of 7.11 mm which was calculated analytically. The resulting model is analysed however, the calculated wall thickness is too thin to withstand the stresses induced into the bottom. Especially in the transition of the two different radii very high stresses of 853.61 N/mm² form and surpass the material properties of a maximum of 482 N/mm². In order to make the elliptical bottom withstand the stresses the thickness is enlarged until the obtained stresses in FEM approximate the material data. The last iteration of the elliptical bottom resulted in a wall thickness of 14.2 mm. With this wall thickness, the new design can withstand the internal pressure with a material safety margin of 1.26% to the maximum obtained equivalent stresses of 472.65 N/mm².
Regarding that both analysed bottoms proved to be adequate to hold this pressure finally, the conclusion can be drawn by the structure mass and integrability. The integration shows the same issues as with the torispherical bottom where the needed extra thickened cylindrical part before the curvature is not integrable to the lower wall thickness of the main cylindrical structure. The total mass of the elliptical bottom including the necessary, enlarged cylindrical part is at 10.31 kg whereas the half-sphere bottom lies at only 6.14 kg and therefore is an appealing choice. Concerning the needed build volume, the half-sphere bottom needs a higher volume than the elliptical bottom but the integration difficulties and the higher mass of the elliptical bottom clearly favour the half-sphere bottom. Therefore, it can be concluded that the half-sphere bottom is the design of choice.

4.2.3 Analysis of the Flanges

This section is dedicated to the evaluation of the flanges needed on the tank. First, the main flange to open the tank, insert the piston and perform maintenance is analysed. Second, the smaller flanges connecting the adapter plates on the top and bottom are discussed. The cylindrical wall thickness of 8.18 mm is kept, as well as the half-sphere bottom. A few technical standards are currently available for flanges and two are taken into consideration: DIN 13445 and DIN 1591. The downside of these standards is, that they are all for validation of results and therefore need an iterative development approach. DIN 1591 also takes leak tightness into consideration whereas the DIN 13445 focusses only on the stability. The calculations of both standards are based on a direct line of force through the seal. Only DIN 1591-3 takes metal to metal contact flanges into consideration, the type chosen to be used in the presented gel propellant tank. Since DIN 1591-3 already needs very precise information about sealing and it is not sufficient to use simple values found in the adjacent table to this standard, it is not taken into consideration. Therefore no useful technical standard was found to validate the results.

In order to design the flange, first the screw forces are calculated and implemented. Therefore, the calculated maximum screw forces reach up to 145.9 kN with M18 12.9 screws. In order to determine the smallest bolt hole circle for the screws, the size of a socket wrench, needed for mounting the nuts is researched and found to have a maximum external diameter of 39 mm. Thus it needs to be assured that there is enough space between each screw to use the tool to mount screws and nuts. With this requirement, a maximum of 45 M18 screws can be placed with a bolt circle of 480 mm close to the tank wall. The iterations mainly changed the flange leaf sizes, however only the final iteration is discussed. The final iteration has a flange leaf thickness of 30 mm each, with a combined thickness of 60 mm. A radius of 1 mm is added in the flange corners in order to help to reduce potential stresses. Also washer rings are used since the screw contact forces exceed the aluminium's strength. As it can be seen in Figure 4, the result shows moderate stresses, and low deformation or opening. In comparison to a previous iteration with very big flange leafs of 50 mm which had a very low deformation but high mass, the 30 mm flange leafs prove to be a very good compromise.

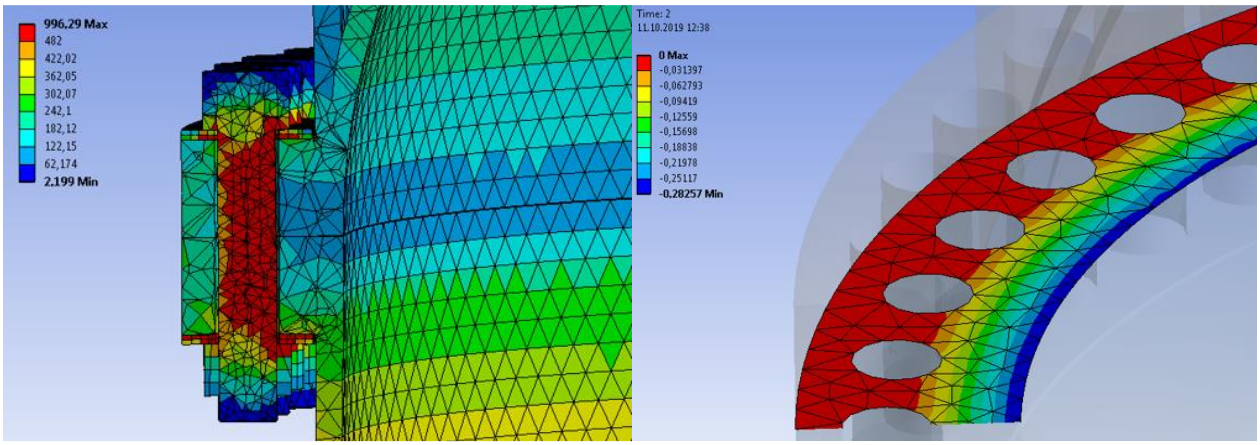

Figure 4: General stresses on the left and resulting gap on the right

The challenge is to find a balance between stiffness and mass. The less stiff the flange is, the higher the deformation gets resulting in higher bending moments. Additionally, the gap that forms gets bigger for less stiff flanges. With the found flange thickness, the resulting stresses in the aluminium are still all far below the critical stress, the screws are calculated before and prove to be sufficient. Also, the gap with 0.28 mm is just slightly bigger than with an almost doubled flange thickness of a previous iteration.

4.2.4 Analysis of the top and bottom Flange

The top and bottom flanges are identical and serve as an option to open the tank and to fit adapter plates for all kinds of connectors. This flange, due to the smaller diameter, experiences much less force than the main flange. Therefore, the required screws were calculated to 20 M8 10.9 screws with a maximum screw utilisation of 80.4 %. Even though the contact pressure between screw heads and the aluminium adapter plate are below the maximum allowed pressure of the aluminium alloy, washer plates are used in order to not damage the material. The principle of numerical simulation is the same as in the previous sections. In the following Figure 5 the results are shown.
It can be seen that the stresses are all well in the range of the used materials. Stresses that surpass the ability of the aluminium are only found in the bolts which are out of steel and are validated before in the calculations. Also with a maximum gap of 0.18 mm this design proves already to be a good option. Following, a convergence study is made, similar to the other flange as before which shows good results.

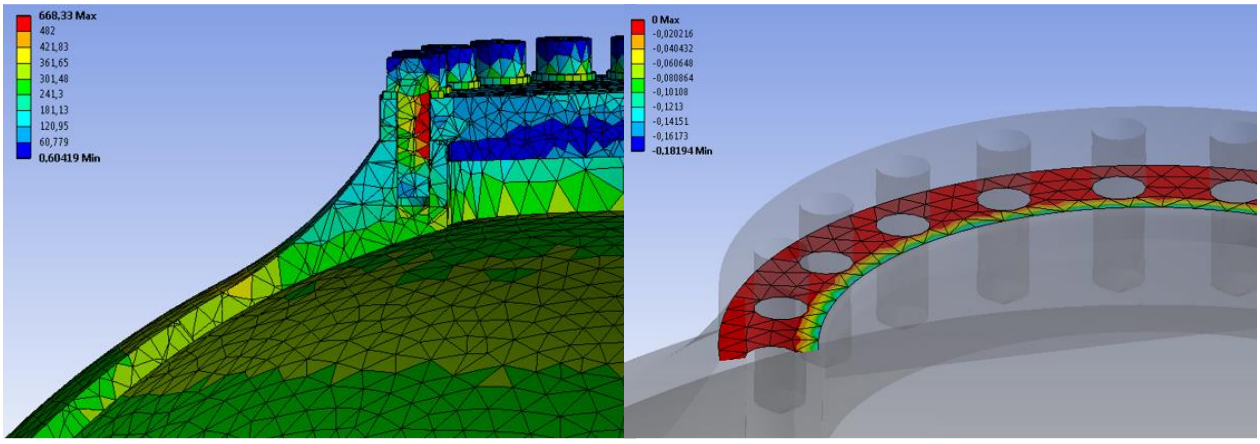

Figure 5: Top/bottom flange: General stresses on the left and resulting gap on the right

4.3 Validation of the final Model

For the final model all previously analysed and chosen parts except for the piston are combined. First the loads that provoke tensile as well as shear stresses and secondly the loads that provoke compressive stresses are applied. The analysis of compressive stresses shows the safety against buckling and the safety against compressive yield, whereas the tensile stresses are analysed for safety against tensile yield as well as tensile ultimate. In addition with the transversal force and the de-spin moment, a check against flange movement in the worst case is performed. The applied loads are shown in the Table 2 in chapter 2.2. The second case represents the normal flight during booster burn although it is a conservative approach because the loads will not act at the same time since the de-spin is triggered much later when the bending moment and transverse force already diminish.

4.3.1 Analysis of tensile Stresses of the final Model

As expected, the maximum stresses are much lower compared to the first load case of only internal pressure with the higher load factor. The maximum equivalent tensile stress, lies at 704 N/mm² and is found in the same area as in the flange analysis before, the contact area between nut and steel washer ring. The stresses in the aluminium structure itself are at a much lower level than with the higher design pressure. Due to the applied bending moment the gap is highly dependent on the direction of the applied moment since it shows a maximum of 0.18 mm on one side and a maximum of 0.086 mm on the opposing side. The corresponding factors of safety against tensile yield and ultimate are shown in Table 10 for a couple of critical regions on the structure. The remaining factors of safety already include the load factors and are all greater or very close to than 1.0. The result of the cylinder middle on the inside is within a certain range to the desired result whereas this is accepted. Therefore, the final model shows to be sufficient enough to be able to withstand the critical flight loads provoking tensile stresses.

Load case	**Region**	**SF_Rp02**	**SF_Rm**
1	Top bottom outside	1.11	1.29
	Cylinder middle inside	0.97	1.13
	Lower bottom outside	1,11	1.29
2	Top bottom outside	1.33	1.55
	Cylinder middle inside	1.15	1.35
	Lower bottom outside	1.32	1.54

Table 10: Corresponding factors of safety

4.3.2 Analysis of compressive Stresses of the final Model

The model stays unchanged from the previous analysis except for the loads. The compressive loads are no challenge for the structure which shows very little stresses. The highest stresses are still in the screws with the maximum stress being between a screw head and the washer ring. Besides the compressive stresses, the structure needs to withstand any form of buckling for the mentioned loads. Therefore, a linear eigenvalue buckling analysis is performed in FEM. The model is checked for the first buckling mode. The results show that buckling occurs in the area of the smallest wall thickness which is the skirt holding the Radax connections on top and bottom with a wall thickness of just 4 mm. Nevertheless, the buckling simulation shows a factor against buckling of 20.71. Since 4 mm wall thickness is commonly used in the structural parts of the rocket and usually weaker Aluminium alloys are used, other structural parts will be subject to buckling before the tank.

5. Application of the numerical Results

The CAD model is progressively completed with all the previously described and numerically analysed additions. The final model shown in the following Figure 6.

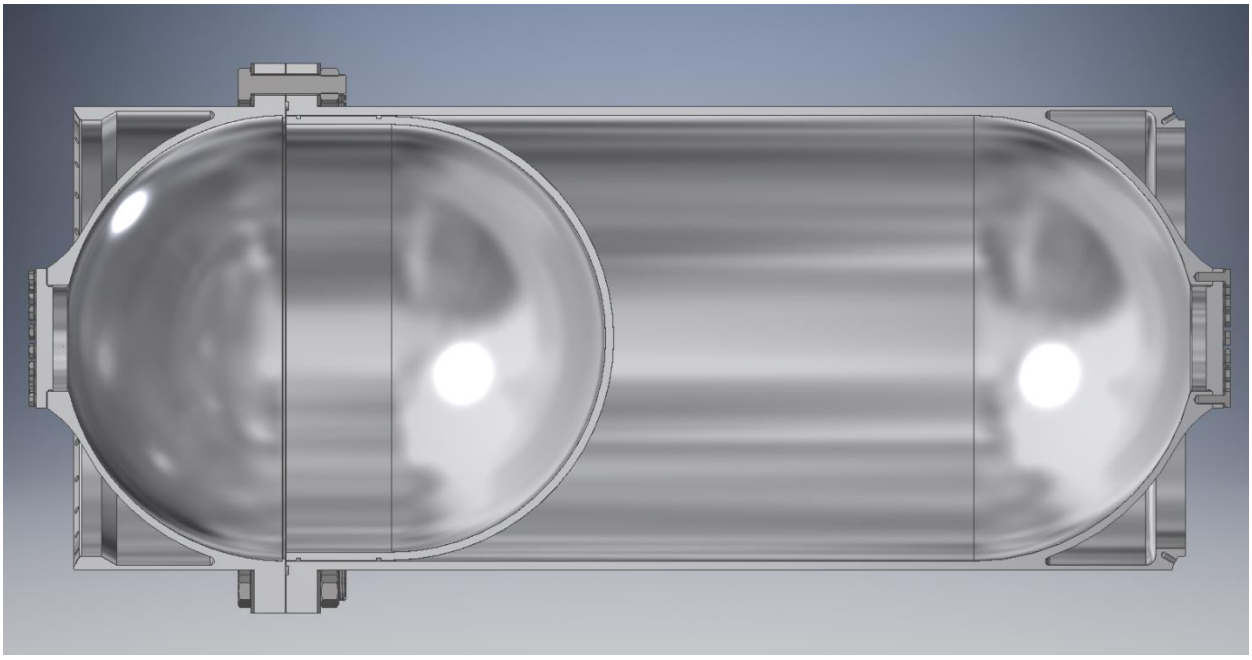

Figure 6: The final CAD model

It shows the basic cylinder design with the half-sphere bottoms, the main flange connecting both main aluminium structures and the flanges on top and bottom to cover the openings and provide an option for the adapter plate. The piston is displayed with a cylindrical part and half-sphere bottom to fit in the tank shape.

5.1 Potential for Optimisation

The gel-powered upper stage is a prototype and many tests like pressure tests, propellant management tests, etc. will have to be performed. It is expected that these tests will show some weaknesses of the design that offer room for optimisation. However a couple of points are already known to have potential for optimisation. The greatest potential to improve the tank is the structural mass. Equation 3 gives the structure efficiency concerning the ability to store fuel with m_{full} as the mass of the tank excluding the piston but including propellant and m_{empty} the empty tank mass.

$$S = \frac{m_{full}}{m_{empty}} = \frac{m_{fuel}+m_{structure}}{m_{structure}} \quad (3)$$

With the resulting tank structure and required propellant mass, the structure ratio is a merely 2.47 with all the necessary additions that are demanded for this prototype, like flanges, bolts and the Radax joints. For comparison, a pressure fed rocket stage is to be chosen. Therefore the EPS, the upper stage of the Ariane 5 is taken into consideration. This stage

is fuelled by 3200 kg monomethylhydrazine and 6500 kg nitrogen tetroxide [12]. It has a total mass including fuel of 10850 kg and an empty mass of 1150 kg [12]. Therefore, the structure factor of the EPS is 9.43 which is much higher than the gel-upper stages factor. However this comparison limps since the EPS tanks are spherical tanks and the used material can be different. Additionally, the used propellant has a different density then the gel propellant. In order to give a benchmark for the tank, the optimum structure factor can be calculated. This is done just with the basic tank structure, without any flanges or joints.

$$e_s = \frac{P*De}{4f} \tag{4}$$

$$e_c = \frac{P*De}{2f} \tag{5}$$

With the lightweight approach of the equation for spherical shapes 4 and cylindrical shapes 5 the volume and mass of the structure can be calculated. The mass of the cylindrical structure is calculated by the following equation 6 and the structure mass of the spherical shape calculates according to equation 7.

$$\mathrm{m_{s,cylinder}} = \mathrm{D\pi e_c L\rho_{structure}} \tag{6}$$

$$\mathrm{m_{s,sphere}} = \mathrm{D^2\pi e_s L\rho_{structure}} \tag{7}$$

For comparison the necessary tank ullage is neglected and the propellant stored in this geometry is calculated by the following equations for the cylindrical and the spherical shapes.

$$\mathrm{m_{f,cylinder}} = \frac{\mathrm{D}^2}{2}\ \mathrm{\pi L\rho_{fuel}} \tag{8}$$

$$\mathrm{m_{f,sphere}} = \frac{\mathrm{D}^3}{2}\ \frac{4}{3}\mathrm{\pi L\rho_{fuel}} \tag{9}$$

With the previous formulas 6, 7, 8 and 9 set in formula 3 this leads to a formulation of the structure factor of:

$$\mathrm{S} = 1 + \frac{\mathrm{f(L+\frac{2}{3}D)}}{\mathrm{2P(L+\frac{1}{2}D)}}\frac{\mathrm{\rho_{fuel}}}{\mathrm{\rho_{structure}}} \tag{10}$$

This equation is plotted two times, one time with a fixed length L and a variable diameter D and another time with the opposite. Using the previously described formulas and parameters leads to the plot shown in Figure 7 on the right with the used values on the left. The blue line represents the structure factor with a variable diameter and a fixed length of 650 mm. The length of 650 mm is the actual final length of the cylindrical tank part. The red line represents the structure factor with a variable length and a fixed diameter of 430 mm which represents the middle diameter of the structure. It can be seen, that the curves have an asymptotic course leading, in this range, to 9.05 for the curve of diameter variation and a maximum of 9.29 for the variation of length. This shows the maximum achievable efficiency in design with this material and this fuel at the given pressure. This however means that the optimum efficiency, which is the highest achieved value in the plot, is found in the red curve in the beginning at zero length. This shows again that spherical tanks, as they are also used in the Ariane 5 upper stage, have the best structure to fuel mass ratio and a favourable.

Parameter	Character	Fixed	Variable	unit
Diameter	D	0.43	0-10	M
Length	L	0.65	0-10	M
Material strength	F	482	-	N/mm²
Internal pressure	P	18	-	N/mm²
Density structure	$\rho_{structure}$	2.8	-	g/cm³
Density fuel	ρ_{fuel}	1.3	-	g/cm³

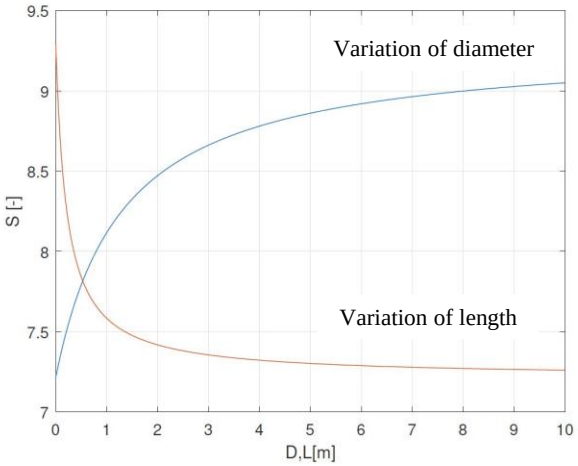

Figure 7: Parameters of the calculation and the Structure factor plotted over the size for the used Aluminium alloy

The designed gel tank without flanges, bolts, etc. reaches a calculated factor of 7.73 which is around 77% of the best achievable factor for the chosen material. Therefore the tank structure itself is designed very efficiently with this material and dimensions. According to Figure 7 great potential for optimisation lies in the use of a different material for the structure, lowering the pressure and maximizing the diameter when minimizing the length. Since lowering of pressure implies the need for a new engine, the recommended factors that can be changed are the choice of material and the tank diameter. When using the previously introduced high strength steel for example a factor of 9.87 is obtained for the current tank dimensions. In comparison this does not seem like a great win, however when looking at other materials like carbon fibre reinforced plastics, factors of 24.46 can be reached. Following Table 11 shows a comparison between some materials.

Material	Ultimate strength N/mm²	Density g/cm³	Structure factor
Aluminium	482	2.8	7.73
Steel	1860	8.2	9.87
Titanium	895	4.45	8.86
CFRP	900	1.5	24.46

Table 11: Structure factor of different materials

Therefore the choice of material can influence the tank structure efficiency significantly. However these options only make sense for an advanced design since then other changes should also be done like inserting the piston and closing the tank ruling out the need for the big flange and heavy screws. According to a manufacturer of hydraulic accumulators, a flexible bladder membrane is no option since the deformation cannot be adapted in a way to push out all the fuel reliably. Therefore the optimisation concerning a larger diameter proves to be difficult when using a piston. Following all the recommended options are listed:

- remove the main flange and the bottom flanges
- extend diameter and lower length
- consider another material

6. Conclusion and Outlook

6.1 Conclusion

This work is part of MORABA's plan to design a new sounding rocket upper stage with a thrust controllable engine. This engine runs on a gelled propellant which is fed from an onboard propellant tank. The aim of this work is to design this tank for a maximum expected operating pressure of 12 MPa as an integral structure of the upper stage. The gel tank features the storing and feeding of propellant during preparation and flight. Since the tank is part of the vehicle primary structure it is designed to withstand the internal pressure as well as flight loads.

With the introduction of the vehicle and mission concept, the adjacent loads and load cases on the tank as well as key design requirements are defined. Since it is an integral structure part it is indispensable to fit a structural interface like the Radax joints to the tank. Other features are included as flanges and adapter plates which are discussed in detail. The relevant technical standards of the ECSS are outlined and load as well as safety factors defined. Additionally the subsystems of the tank as the cylindrical part with its concerning wall thickness, the different bottom types, the feeding principle and more are explained and analytically calculated.

Following the analytical concept development, the numerical FEM simulation is used for the design of the more complex parts of the geometry. Therefore, a simple FEM model is built and verified with the basic analytical calculations of the tanks cylinder and bottom parts. With the validated FEM results, the model is progressively completed with further elements like the flanges etc. The main flange is simulated and a design solution is found iteratively. Finally it is shown, that the tank is sufficient to withstand the loads and load cases present in handling and flight with the required factors of safety. The final model holds the required amount of gelled propellant and is pressurised by a high-pressure gas tank. The gel tank is made of Aluminium, is fitted with a piston and has a dry mass of roughly 80 kg.

6.2 Outlook

Following the work described in this paper the tank is ready for detailed design modifications and testing. Especially the testing is a very significant step in the development process to validate the FEM model. This includes pressure cycle tests, maximum pressure tests until bursting of the structure, leak tests etc. The results will then dictate the further proceeding of potential redesigns over minor changes to structural acceptance of the design. Acceptance of the tank design leads to further system function tests like fuel management and integration tests. Depending on the progress of the project partners, the acceptance of the design can be followed by test firing and hover tests of the entire upper stage propulsion system. Eventually, after the design has proven to be trustworthy it can be used for the actual purpose of flying a research mission. Design optimisation efforts can be conducted, e.g. by using different materials. A carbon fibre overwrap system can be an option since this presents a high margin of improvement concerning the mass shown in the structure factor. Eventually an appropriate bladder or membrane concept can also be found to further reduce structural mass. Concluding, a certain amount of further work is required to bring the system into service or to optimise it, providing many opportunities for interesting scientific and engineering questions to be solved.

List of references

[1] MORABA. Suborbitaler Raumflug mit Höhenforschungsraketen und Ballonen. April 2021 URL: https://www.moraba.de.
[2] Robin H. BRAND. Britain's first space rocket - The story of the Skylark. New Forest Electronics, 2014.
[3] Prof. Dr. M. OSCHWALD. Raumfahrtantriebe I. Deutsches Zentrum für Luft- und Raumfahrt e.V., 2017.
[4] MORABA. We will lift you up! Oct. 2019. URL: https://www.moraba.de.
[5] P. Caldas Pinto K.W. NAUMANN. „Green, Controllable, Safe, Affordable and Mature Gelled Propellant Rocket Motor Technology for Space and Sub-Orbital Launchers". In: AIAA Propulsion and Energy Forum. 2018.
[6] ESA-ESTEC. Space engineering - Structural design and verification of pressurized hardware - ECSS-E-ST-32-02C. ECSS Secretariat, 2008.
[7] Tsutomu Takechi IKUHIRO INAGAKI. Application and Features of Titanium for the Aerospace Industry. In: (2014).
[8] DIN EN 13445-3:2018-12. Normenausschuss Chemischer Apparatebau (FNCA) im DIN.
[9] ASME. ASME Code Section VIII - Division 1. ASME, 2017.
[10] DIN28011. Normenausschuss Chemischer Apparatebau (FNCA) im DIN
[11] Thomas Nelson ERKE WANG. „Back to Elements - Tetrahedra vs. Hexahedra". In: 2004.
[12] Bernd LEITENBERGER. Die Ariane 5. Oct. 2019. URL: https://www.bernd-leitenberger.de/ariane5.shtml.
[13] ESA-ESTEC. Space engineering - Structural design and verification of pressurized hardware - ECSS-E-ST-32-10C Rev.1. ECSS Secretariat, 2009.